Novel risk loci for COVID-19 hospitalization among admixed American populations

Ángel Carracedo on behalf of Spanish COalition to Unlock Research on host GEnetics on COVID-19 (SCOURGE)

Email address for correspondence: angel.carracedo@usc.es

Author list:

https://docs.google.com/document/d/1gJVHCOM59Yczz6BduHfpyOQEmxIXcBXr/edit?usp=sharing&ouid=117105050981428441732&rtpof=true&sd=true

Abstract

The genetic basis of severe COVID-19 has been thoroughly studied and many genetic risk factors shared between populations have been identified. However, reduced sample sizes from non-European groups have limited the discovery of population-specific common risk loci. In this second study nested in the SCOURGE consortium, we have conducted the largest GWAS meta-analysis for COVID-19 hospitalization in admixed Americans, comprising a total of 4,702 hospitalized cases recruited by SCOURGE and other seven participating studies in the COVID-19 Host Genetic Initiative. We identified four genome-wide significant associations, two of which constitute novel loci and first discovered in Latin-American populations (*BAZ2B* and *DDIAS*). A trans-ethnic meta-analysis revealed another novel cross-population risk locus in *CREBBP*. Finally, we assessed the performance of a cross-ancestry polygenic risk score in the SCOURGE admixed American cohort.

Introduction

To date, more than 50 loci associated to COVID-19 susceptibility, hospitalization, and severity have been identified using genome-wide association studies (GWAS)[1,2]. The COVID-19 Host Genetics Initiative (HGI) has made significant efforts[3] to augment the power to identify disease loci by recruiting individuals from diverse populations and conducting a trans-ancestry meta-analysis. Despite this, the lack of genetic diversity and a focus on cases of European ancestries still predominate in the studies[4,5]. Besides, while trans-ancestry meta-analyses are a powerful approach for discovering shared genetic risk variants with similar effects across populations[6], they may fail to identify risk variants that have larger effects on particular underrepresented populations. Genetic disease risk has been shaped by the particular evolutionary history of populations and the environmental exposures[7]. Their action is particularly important for infectious diseases due to the selective constrains that are imposed by the host-pathogen interactions[8,9]. Literature examples of this in COVID-19 severity includes a *DOCK2* gene variant in East Asians[10], and frequent loss of function variants in *IFNAR1* and *IFNAR2* genes in Polynesian and Inuit populations, respectively[11,12].

Including diverse populations in case-control GWAS studies with unrelated participants usually require a prior classification of individuals in genetically homogeneous groups, which are typically analysed separately to control the population stratification effects[13]. Populations with recent admixture impose an additional challenge to the GWAS due to their complex genetic diversity and linkage disequilibrium (LD) patterns, requiring the development of alternative approaches and a careful inspection of results to reduce the false positives due to population structure[7]. In fact, there are benefits in study power from modelling the admixed ancestries either locally, at regional scale in the chromosomes, or globally, across the genome, depending on factors such as the heterogeneity of the risk variant in frequencies or the effects among the ancestry

strata[14]. Despite the development of novel methods specifically tailored for the analysis of admixed populations[15], the lack of a standardized analysis framework and the difficulties to confidently cluster the admixed individuals into particular genetic groups often leads to their exclusion from GWAS.

The Spanish Coalition to Unlock Research on Host Genetics on COVID-19 (SCOURGE) recruited COVID-19 patients between March and December 2020 from hospitals across Spain and from March 2020 to July 2021 in Latin-America (https://www.scourge-covid.org). A first GWAS of COVID-19 severity among Spanish patients of European descent revealed novel disease loci and explored age and sex varying effects of the genetic factors[16]. Here we present the findings of a GWAS meta-analysis in admixed American (AMR) populations, comprising individuals from the SCOURGE Latin-American cohort and the HGI studies, which allowed to identify two novel severe COVID-19 loci, *BAZ2B* and *DDIAS*. Further analyses modelling the admixture from three genetic ancestral components and performing a trans-ethnic meta-analysis led to the identification of an additional risk locus near *CREBBP*. We finally assessed a cross-ancestry polygenic risk score model with variants associated with critical COVID-19.

Results

Meta-analysis of COVID-19 hospitalization in admixed Americans

Study cohorts

Within the SCOURGE consortium, we included 1,608 hospitalized cases and 1,887 controls (not hospitalized COVID-19 patients) from Latin-American countries and from recruitments of individuals of Latin-American descend conducted in Spain (Supplementary Table 1). Quality control details and estimation of global genetic

inferred ancestry (GIA) (supplementary Figure 1) are described in Methods, whereas clinical and demographic characteristics of patients included in the analysis are shown in Table 1. Summary statistics from the SCOURGE cohort were obtained under a logistic mixed model with the SAIGE model (Methods). Another seven studies participating in the COVID-19 HGI consortium were included in the meta-analysis of COVID-19 hospitalization in admixed Americans (Figure 1).

GWAS meta-analysis

We performed a fixed-effects GWAS meta-analysis using the inverse of the variance as weights for the overlapping markers. The combined GWAS sample size consisted of 4,702 admixed AMR hospitalized cases and 68,573 controls.

This GWAS meta-analysis revealed genome-wide significant associations at four risk loci (Table 2, Figure 2), two of which (*BAZ2B* and *DDIAS*) were novel discoveries. Variants of these loci were prioritized by positional and expression quantitative trait loci (eQTL) mapping with FUMA, identifying four lead variants linked to other 310 variants and 31 genes (Supplementary Tables 2-4). A gene-based association test revealed a significant association in *BAZ2B* and in previously known COVID-19 risk loci: *LZTFL1*, *XCR1*, *FYCO1*, *CCR9*, and *IFNAR2* (Supplementary Table 5).

Located within the gene *BAZ2B*, the sentinel variant rs13003835 is an intronic variant associated with an increased risk of COVID-19 hospitalization (Odds Ratio [OR]=1.20, 95% Confidence Interval [CI]=1.12-1.27, $p=3.66x10^{-8}$). This association was not previously reported in any GWAS of COVID-19 published to date. Interestingly, rs13003835 did not reach significance (p=0.972) in the COVID-19 HGI trans-ancestry meta-analysis including the five population groups[1]. Based on our mapping strategy (see Methods), we also prioritized *PLA2R1*, *LY75*, *WDSUB1*, and *CD302* in this locus.

The other novel risk locus is led by the sentinel variant rs77599934, a rare intronic variant located in chromosome 11 within *DDIAS* and associated with risk of COVID-19 hospitalization (OR=2.27, 95%CI=1.70-3.04, $p=2.26x10^{-8}$). The *PRCP* gene was an additional prioritized gene at this locus.

We also observed a suggestive association with rs2601183 in chromosome 15, which is located between *ZNF774* and *IQGAP1* (allele-G OR=1.20, 95%CI=1.12-1.29, $p=6.11x10^{-8}$, see Supplementary Table 2), which has not yet been reported in any other GWAS of COVID-19 to date. This sentinel variant is in perfect LD ($r^2=1$) with rs601183, an eQTL of *ZNF774* in the lung.

The GWAS meta-analysis also pinpointed two significant variants at known loci, *LZTFL1* and *FOXP4*. The SNP rs35731912 was previously associated with COVID-19 severity in EUR populations[17], and it was mapped to *LZTFL1*. As for rs2477820, while it is a novel risk variant within gene *FOXP4*, it has a moderate LD ($r^2=0.295$) with rs2496644, which has been linked to COVID-19 hospitalization[18]. This is consistent with the effects of LD in tag-SNPs when conducting GWAS in diverse populations.

Functional mapping of novel risk variants

Bayesian fine mapping

We performed different approaches to narrow down the prioritized loci to a set of most probable genes driving the associations. First, we computed credible sets at the 95% confidence for causal variants and annotated them with VEP and the V2G aggregate scoring (Supplementary Table 6, Supplementary Figure 3). The 95% confidence credible set from the region of chromosome 2 around rs13003835 included 76 variants. However, the approach was unable to converge allocating variants in a 95% confidence credible set for the region in chromosome 11.

Colocalization of eQTLs

To determine if the novel genetic risk loci were associated with gene expression in relevant tissues (whole blood, lung, lymphocytes, and oesophagus mucosa), we computed the posterior probabilities (PP) of colocalization for overlapping variants allocated to the 95% confidence credible set. We used the GTEx v8 tissues as the main expression dataset, although it is important to consider that the eQTL associations were carried out mainly on individuals of EUR ancestries. To confirm the colocalization in other ancestries, we also performed analyses on three expression datasets computed on admixed AMR, leveraging data from individuals with high African GIA, high Native-American ancestry, and from a pooled cohort (Methods). Results are shown in the supplementary Table 7.

Five genes (*LY75*, *BAZ2B*, *CD302*, *WDSUB1*, and *PLA2R1*) were the candidates for eQTL colocalization in the associated region in chromosome 2. However, *LY75* emerged as the most likely causal gene for this locus since the colocalization in whole blood was supported with a PP for H4 (PPH4) of 0.941 and with robust results (supplementary Figure 4). Moreover, this also allowed to prioritize rs12692550 as the most probable causal variant for both traits at this locus with a PP_SNP_H4 of 0.74. Colocalization with gene expression data from admixed AMR validated this finding. *LY75* also had evidence of colocalization in lungs (PPH4=0.887) and the esophagus mucosa (PPH4=0.758). However, we could not prioritize a single causal variant in these two other tissues and sensitivity analyses revealed a weak support.

CD302 and *BAZ2B* were the second and third most likely genes that could drive the association, respectively, according to the colocalization evidence. *CD302* was the most probable according to the high AFR genetic ancestries dataset (supplementary Figure 5).

Despite the chromosome 11 region failing to colocalize with gene expression associations for any of the tissues, the lead variant rs77599934 is in moderate-to-strong LD (r^2=0.776) with rs60606421, which is an eQTL associated to a reduced expression of *DDIAS* in the lungs (supplementary Figure 6). The highest PPH4 for *DDIAS* was in the high AFR genetic ancestry expression dataset (0.71).

Transcriptome-wide association study (TWAS)

Five novel genes, namely *SLC25A37*, *SMARCC1*, *CAMP*, *TYW3*, and *S100A12* (supplementary Table 8) were found significantly associated in the cross-tissue TWAS. To our knowledge, these genes have not been reported previously in any COVID-19 TWAS or GWAS analyses published to date. In the single tissue analyses, *ATP5O* and *CXCR6* were significantly associated in lungs, *CCR9* was significantly associated in whole blood, and *IFNAR2* and *SLC25A37* were associated in lymphocytes.

Likewise, we carried out the TWAS analyses using the models trained in the admixed populations. However, no significant gene-pairs were detected in this case. The 50 genes with the lowest p-values are shown in the supplementary Table 9.

Genetic architecture of COVID-19 hospitalization in AMR populations

Allele frequencies of rs13003835 and rs77599934 across ancestries

Neither rs13003835 (*BAZ2B*) or rs77599934 (*DDIAS*) were significantly associated in the COVID-19 HGI B2 cross-population or population-specific meta-analyses. Thus, we investigated their allele frequencies (AF) across populations and compared their effect sizes.

According to gnomAD v3.1.2, the T allele at rs13003835 (*BAZ2B*) has an AF of 43% in admixed AMR groups while AF is lower in the EUR populations (16%) and in the

global sample (29%). Local ancestry inference (LAI) reported by gnomAD shows that within the Native-American component, the risk allele T is the major allele, whereas it is the minor allele within the African and European LAI components. These large differences in AF might be the reason underlying the association found in AMR populations. However, when comparing effect sizes between populations, we found that they were in opposite direction between SAS-AMR and EUR-AFR-EAS and that there was a large heterogeneity among them (Figure 3).

rs77599934 (*DDIAS*) had an AF of 1.1% for the G allele in the non-hospitalized controls (Table 2), in line with the recorded gnomAD AF of 1% in admixed AMR groups. This variant has potential to be population-specific variant, given the allele frequencies in other population groups such as EUR (0% in Finnish, 0.025% in non-Finnish), EAS (0%) and SAS (0.042%) and its greater effect size over AFR populations (Figure 3). Examining the LAI, the G allele occurs at 1.1% frequency in the African component while it is almost absent in the Native-American and European. Due to its low MAF, rs77599934 was not analyzed in the COVID-19 HGI B2 cross-population meta-analysis and was only present in the HGI B2 AFR population-specific meta-analysis, precluding the comparison (Figure 3). For this reason, we retrieved the variant with the lowest p-value within a 50 kb region around rs77599934 in the COVID-19 HGI cross-population analysis to investigate if it was in moderate-to-strong LD with our sentinel variant. The variant with the smallest p-value was rs75684040 (OR=1.07, 95%CI=1.03-1.12, $p=1.84x10^{-3}$). Yet, LD calculations using the 1KGP phase 3 dataset indicated that rs77599934 and rs75684040 were poorly correlated ($r^2=0.11$).

Cross-population meta-analyses

We carried out two cross-ancestry inverse variance-weighted fixed-effects meta-analyses with the admixed AMR GWAS meta-analysis results to evaluate whether the

discovered risk loci replicated when considering other population groups. In doing so, we also identified novel cross-population COVID-19 hospitalization risk loci.

First, we combined the SCOURGE Latin American GWAS results with the HGI B2 ALL analysis (supplementary Table 10). We refer to this analysis as the SC-HGI$_{ALL}$ meta-analysis. Out of the 40 genome-wide significant loci associated with COVID-19 hospitalization in the last HGI release[1], this study replicated 39 and the association was stronger than in the original study in 29 of those (supplementary Table 11). However, the variant rs13003835 located in *BAZ2B* did not replicate (OR=1.00, 95%CI=0.98-1.03, p=0.644).

In this cross-ancestry meta-analysis, we replicated two associations that were not found in HGIv7 albeit they were sentinel variants in the latest GenOMICC meta-analysis[2]. We found an association at the *CASC20* locus led by the variant rs2876034 (OR=0.95, 95%CI=0.93-0.97, p=2.83x10^{-8}). This variant is in strong LD with the sentinel variant of that study (rs2326788, r^2=0.92), which was associated with critical COVID-19[2]. Besides, this meta-analysis identified the variant rs66833742 near *ZBTB7A* associated with COVID-19 hospitalization (OR=0.94, 95%CI=0.92-0.96, p=2.50x10^{-8}). Notably, rs66833742 or its perfect proxy rs67602344 (r^2=1) are also associated with upregulation of *ZBTB7A* in whole blood and in esophagus mucosa. This variant was previously associated with COVID-19 hospitalization[2].

In a second analysis, we also explored the associations across the defined admixed AMR, EUR, and AFR ancestral sources by combining through meta-analysis the SCOURGE Latin American GWAS results with the HGI studies in EUR, AFR, and admixed AMR, and excluding those from EAS and SAS (Supplementary Table 12). We refer to this as the SC-HGI$_{3POP}$ meta-analysis. The association at rs13003835 (*BAZ2B*, OR=1.01, 95%CI=0.98-1.03, p=0.605) was not replicated and rs77599934 near *DDIAS*

could not be assessed, although the association at the *ZBTB7A* locus was confirmed (rs66833742, OR=0.94, 95%CI=0.92-0.96, $p=1.89x10^{-8}$). The variant rs76564172 located near *CREBBP* also reached statistical significance (OR=1.31, 95% CI=1.25-1.38, $p=9.64x10^{-9}$). The sentinel variant of the region linked to *CREBBP* (in the trans-ancestry meta-analysis) was also subjected a Bayesian fine mapping (supplementary Table 6) and colocalization with eQTLs under the GTEx v8 MASHR models in lungs, esophagus mucosa, whole blood, and transformed lymphocytes. Eight variants were included in the credible set for the region in chromosome 16 (meta-analysis SC-HGI_{3POP}), although *CREBBP* did not colocalize in any of the tissues.

Polygenic risk score models

Using the 49 variants associated with disease severity that are shared across populations according to the HGIv7, we constructed a polygenic risk score (PGS) model to assess its generalizability in the admixed AMR (Supplementary Table 13). First, we calculated the PGS for the SCOURGE Latin Americans and explored the association with COVID-19 hospitalization under a logistic regression model. The PGS model was associated with a 1.48-fold increase in COVID-19 hospitalization risk per every PGS standard deviation. It also contributed to explain a slightly larger variance (R2=1.07%) than the baseline model.

Subsequently, we divided the individuals into PGS deciles and percentiles to assess their risk stratification. The median percentile among controls was 40, while in cases it was 63. Those in the top PGS decile exhibited a 5.90-fold (95% CI=3.29-10.60, $p=2.79x10^{-9}$) greater risk compared to individuals in the lowest decile, whereas the effects for the rest of the comparisons were much milder.

We also examined the distribution of PGS scores across a 5-level severity scale to further determine if there was any correspondence between clinical severity and genetic risk. Median PGS scores were lower in the asymptomatic and mild groups, whereas higher median scores were observed in the moderate, severe, and critical patients (Figure 4). We fitted a multinomial model using the asymptomatic class as reference and calculated the OR for each category (Supplementary Table 13), observing that the disease genetic risk was similar among asymptomatic, mild, and moderate patients. Given that the PGS was built with variants associated with critical disease and/or hospitalization and that the categories severe and critical correspond to hospitalized patients, these results underscore the ability of cross-ancestry PGS for risk stratification even in an admixed population.

Finally, we incorporated the novel lead SNPs from our AMR meta-analysis (rs13003835, rs2477820, and rs77599934) into the PGS model. Their inclusion in the model contributed to explain a larger variance (R2=1.74%) than the model without them. This result, however, should be taken with caution given the risk of overfitting due to the use of the same subjects both for the derivation and testing of the variants.

DISCUSSION

We have conducted the largest GWAS meta-analysis of COVID-19 hospitalization in admixed AMR to date. While the genetic risk basis discovered for COVID-19 is largely shared among populations, trans-ancestry meta-analyses on this disease have primarily included EUR samples. This dominance of GWAS in Europeans, and the subsequent bias in sample sizes, can mask population-specific genetic risks (i.e., variants that are monomorphic in some populations) or be less powered to detect risk variants having

higher allele frequencies in population groups other than Europeans. In this sense, after combining data from admixed AMR patients, we found two risk loci which are first discovered in a GWAS of Latin-American populations. Interestingly, the sentinel variant rs77599934 in the *DDIAS* gene is a rare coding variant (~1% for allele G) with a large effect on COVID-19 hospitalization that is nearly monomorphic in most of the other populations. This has likely led to its exclusion from the cross-populations meta-analyses conducted to date, remaining undetectable.

Fine mapping of the region harbouring *DDIAS* did not reveal further information about which gene could be the more prone to be causal, or about the functional consequences of the risk variant. However, *DDIAS*, known as damage-induced apoptosis suppressor gene, is itself a plausible candidate gene. It has been linked to DNA damage repair mechanisms: research showed that depletion of *DDIAS* led to an increase of ATM phosphorylation and the formation of p53-binding protein (53BP1) foci, a known biomarker of DNA double-strand breaks, suggesting a potential role in double-strand break repair[19]. Similarly, elevated levels of phosphorylated nuclear histone 2AXγ were detected after knocking down *DDIAS*, further emphasizing its role in DNA damage[20]. Interestingly, a study found that the infection by SARS-CoV-2 also triggered the phosphorylation of the ATM kinase and inhibited repair mechanisms, causing the accumulation of DNA damage[21]. This same study reported the activation of the pro-inflammatory pathway p38/MAPK by the virus, which was as well prompted after knocking-down *DDIAS*[20].

Regarding lung function, the role of *DDIAS* in lung cancer has been widely studied. It has been proposed as a potential biomarker for lung cancer after finding that it interacts with STAT3 in lung cancer cells, regulating IL-6[22,23] and thus mediating inflammatory processes. Furthermore, another study determined that its blockade inhibited lung

cancer cell growth[20]. The sentinel variant was in strong LD with an eQTL that reduced gene expression of *DDIAS* in lung, and our findings suggest that *DDIAS* gene may be indeed involved in viral response. Hence, one reasonable hypothesis is that reduced expression of *DDIAS* could potentially facilitate SARS-CoV-2 infection through the downregulation of pathways involved in DNA repairment and inflammation. Another prioritized gene from this region was *PRCP*, an angiotensinase that has been linked to hypertension and for which a hypothesis on its role on COVID-19 progression has been raised[24,25].

The risk region found in chromosome 2 prioritized more than one gene. The lead variant rs13003835 is located within *BAZ2B*. *BAZ2B* encodes one of the regulatory subunits of the Imitation switch (ISWI) chromatin remodelers[26] constituting the BRF-1/BRF-5 complexes with SMARCA1 and SMARCA5, respectively, and the association signal colocalized with eQTLs in whole blood. The gene *LY75* (encoding the lymphocyte antigen 75) also colocalized with eQTLs in whole blood, esophagus mucosa, and lung tissues. Lymphocyte antigen 75 is involved in immune processes through antigen presentation in dendritic cells and endocytosis[27], and has been associated with inflammatory diseases, representing also a compelling candidate for the region. Increased expression of *LY75* has been detected within hours after the infection by SARS-CoV-2[28,29]. Lastly, the signal of *CD302* colocalized in individuals with high AFR ancestral admixture in whole blood. This gene is located in the vicinity of *LY75* and both conform the readthrough LY75-CD302. It is worth noting that differences in AF for this variant suggest that analyses in AMR populations might be more powered to detect the association, supporting the necessity of population-specific studies.

A third novel risk region was observed in chromosome 15, between the genes *IQGAP1* and *ZNF774*, although not reaching genome-wide significance.

Secondary analyses revealed five TWAS-associated genes, some of which have been already linked to severe COVID-19. In a comprehensive multi-tissue gene expression profiling study[30], decreased expression of *CAMP* and *S100A8*/*S100A9* genes in COVID-19 severe patients was observed, while another study detected the upregulation of *SCL25A37* among severe COVID-19 patients[31]. *SMARCC1* is a subunit of the SWI/SNF chromatin remodelling complex that has been identified as pro-viral for SARS-CoV-2 and other coronavirus strains through a genome-wide screen[32]. This complex is crucial for *ACE2* expression and the viral entry in the cell[33].

To explore the genetic architecture of the trait among admixed AMR populations, we performed two cross-ancestry meta-analyses including the SCOURGE Latin-American cohort GWAS findings. We found that the two novel risk variants did not associate with COVID-19 hospitalization outside the population-specific meta-analysis, highlighting the importance of complementing trans-ancestry meta-analyses with group-specific analyses. Notably, this analysis did not replicate the association at the *DSTYK* locus, which was associated with severe COVID-19 in Brazilian individuals with higher European admixture[34]. This lack of replication supports the initial hypothesis of that study suggesting that the risk haplotype derived from European populations, as we have reduced the weight of this ancestral contribution in our study by excluding those individuals.

Moreover, these cross-ancestry meta-analyses pointed to three loci that were not genome-wide significant in the HGIv7 ALL meta-analysis: a novel locus at *CREBBP*, and two loci at *ZBTB7A* and *CASC20* that were reported in another meta-analysis. *CREBBP* and *ZBTB7A* achieved a stronger significance when considering only EUR, AFR, and admixed AMR GIA groups. According to a recent study, elevated levels of the *ZBTB7A* gene promote a quasi-homeostatic state between coronaviruses and host

cells, preventing cell death by regulating oxidative stress pathways[35]. This gene is involved in several signalling pathways, such as B and T cell differentiation[36]. On a separate note, *CREBBP* encodes the CREB binding protein (CBP), involved in transcription activation, that is known to positively regulate the type I interferon response through virus-induced phosphorylation of IRF-3[37]. Besides, the CREBP/CBP interaction has been implicated in SARS-CoV-2 infection[38] via the cAMP/PKA pathway. In fact, cells with suppressed *CREBBP* gene expression exhibit reduced replication of the so called Delta and Omicron SARS-CoV-2 variants[38].

The cross-population PGS model effectively stratified individuals based on their genetic risk and demonstrated consistency with the clinical severity classification of the patients. The inclusion of the new variants in the PGS model slightly improved the predictive value of the PGS. However, it is important to confirm this last finding in an external admixed AMR cohort to address potential overfitting arising from using the same individuals both for the discovery of the associations and for testing the model.

This study is subject to limitations, mostly concerning the sample recruitment and composition. The SCOURGE Latino-American sample size is small and the GWAS is underpowered. Another limitation is the difference in case-control recruitment across sampling regions that, yet controlled for, may reduce the ability to observe significant associations driven by different compositions of the populations. In this sense, the identified risk loci might not replicate in a cohort lacking any of the parental population sources from the three-way admixture. Likewise, we could not explicitly control for socio-environmental factors that could have affected COVID-19 spread and hospitalization rates, although genetic principal components are known to capture non-genetic factors. Finally, we must acknowledge the lack of a replication cohort. We have used all the available GWAS data for COVID-19 hospitalization in admixed AMR in

this meta-analysis due to the low number of studies conducted. Therefore, we had no studies to replicate or validate the results. These concerns may be addressed in the future by including more AMR GWAS studies in the meta-analysis, both by involving diverse populations in study designs and by supporting research from countries in Latin-America.

This study provides novel insights into the genetic basis of COVID-19 severity, emphasizing the importance of considering host genetic factors through using non-European populations, especially of admixed sources. Such complementary efforts can pin down new variants and increase our knowledge on the host genetic factors of severe COVID-19.

Materials and methods

GWAS in Latin Americans from SCOURGE

The SCOURGE Latin American cohort

A total of 3,729 of COVID-19 positive cases were recruited across five countries from Latin America (Mexico, Brazil, Colombia, Paraguay, and Ecuador) by 13 participating centres (supplementary Table 1) from March 2020 to July 2021. In addition, we included 1,082 COVID-19 positive individuals recruited between March and December 2020 in Spain who either had evidence of origin from a Latin American country or showed inferred genetic admixture between AMR, EUR, and AFR (with < 0.05% SAS/EAS). These individuals were excluded from a previous SCOURGE study that focused on participants with European genetic ancestries[16]. We used hospitalization as a proxy for disease severity and defined as cases those COVID-19 positive patients that underwent hospitalization as a consequence of the infection and used as controls those that did not need hospitalization due to COVID-19.

Samples and data were collected with informed consent after the approval of the Ethics and Scientific Committees from the participating centres and by the Galician Ethics Committee Ref 2020/197. Recruitment of patients from IMSS (in Mexico, City), was approved by of the National Comitte of Clinical Research, from Instituto Mexicano del Seguro Social, Mexico (protocol R-2020-785-082).

Samples and data were processed following normalized procedures. The REDCap electronic data capture tool[39,40], hosted at Centro de Investigación Biomédica en Red (CIBER) from the Instituto de Salud Carlos III (ISCIII), was used to collect and manage demographic, epidemiological, and clinical variables. Subjects were diagnosed for COVID-19 based on quantitative PCR tests (79.3%), or according to clinical (2.2%) or laboratory procedures (antibody tests: 16.3%; other microbiological tests: 2.2%).

SNP array genotyping

Genomic DNA was obtained from peripheral blood and isolated using the Chemagic DNA Blood 100 kit (PerkinElmer Chemagen Technologies GmbH), following the manufacturer's recommendations.

Samples were genotyped with the Axiom Spain Biobank Array (Thermo Fisher Scientific) following the manufacturer's instructions in the Santiago de Compostela Node of the National Genotyping Center (CeGen-ISCIII; http://www.usc.es/cegen). This array contains probes for genotyping a total of 757,836 SNPs. Clustering and genotype calling were performed using the Axiom Analysis Suite v4.0.3.3 software.

Quality control steps and variant imputation

A quality control (QC) procedure using PLINK 1.9[41] was applied to both samples and the genotyped SNPs. We excluded variants with a minor allele frequency (MAF) <1%, a call rate <98%, and markers strongly deviating from Hardy-Weinberg equilibrium

expectations ($p<1x10^{-6}$) with mid-p adjustment. We also explored the excess of heterozygosity to discard potential cross-sample contaminations. Samples missing >2% of the variants were filtered out. Subsequently, we kept the autosomal SNPs and removed high LD regions and conducted LD-pruning (windows of 1,000 SNPs, with step size of 80 and r^2 threshold of 0.1) to assess kinship and estimate the global ancestral proportions. Kinship was evaluated based on IBD values, removing one individual from each pair with PI_HAT>0.25 that showed a Z0, Z1, and Z2 coherent pattern (according to the theoretical expected values for each relatedness level). Genetic principal components (PCs) were calculated with PLINK with the subset of LD pruned variants.

Genotypes were imputed with the TOPMed version r2 reference panel (GRCh38) using the TOPMed Imputation Server and variants with Rsq<0.3 or with MAF<1% were filtered out. A total of 4,348 individuals and 10,671,028 genetic variants were included in the analyses.

Genetic admixture estimation

Global genetic inferred ancestry (GIA), referred to the genetic similarity to the used reference individuals, was estimated with the ADMIXTURE[42] v1.3 software following a two-step procedure. First, we randomly sampled 79 European (EUR) and 79 African (AFR) samples from The 1000 Genomes Project (1KGP)[43] and merged them with the 79 Native American (AMR) samples from Mao et al.[44] keeping the biallelic SNPs. LD-pruned variants were selected from this merge using the same parameters as in the QC. We then run an unsupervised analysis with K=3 to redefine and homogenize the clusters and to compose a refined reference for the analyses, by applying a threshold of ≥95% of belonging to a particular cluster. As a result of this, 20 AFR, 18 EUR, and 38 AMR

individuals were removed. The same LD-pruned variants data from the remaining individuals were merged with the SCOURGE Latin American cohort to perform a supervised clustering and estimated admixture proportions. A total of 471 samples from the SCOURGE cohort with >80% estimated European GIA were removed to reduce the weight of the European ancestral component, leaving a total of 3,512 admixed American (AMR) subjects for downstream analyses.

Association analysis

Results for the SCOURGE Latin Americans GWAS were obtained testing for COVID-19 hospitalization as a surrogate of severity. To accommodate the continuum of GIA in the cohort, we opted for a joint testing of all the individuals as a single study using a mixed regression model, as this approach has demonstrated a greater power and to sufficiently control population structure[45]. The SCOURGE cohort consisted of 3,512 COVID-19 positive patients: cases (n=1,625) were defined as hospitalized COVID-19 patients and controls (n=1,887) as non-hospitalized COVID-19 positive patients.

Logistic mixed regression models were fitted using the SAIGEgds[46] package in R, which implements the two-step mixed SAIGE[47] model methodology and the SPA test. Baseline covariables included sex, age, and the first 10 PCs. To account for a potential heterogeneity in the recruitment and hospitalization criteria across the participating countries, we adjusted the models by groups of the recruitment areas classified in six categories: Brazil, Colombia, Ecuador, Mexico, Paraguay, and Spain. This dataset has not been used in any previously GWAS of COVID-19 published to date.

Meta-analysis of Latin-American populations

The results of the SCOURGE Latin American cohort were meta-analyzed with the AMR HGI-B2 data, conforming our primary analysis. Summary results from the HGI

freeze 7 B2 analysis corresponding to the admixed AMR population were obtained from the public repository (April 8, 2022: https://www.covid19hg.org/results/r7/), summing up 3,077 cases and 66,686 controls from seven contributing studies. We selected the B2 phenotype definition because it offered more power and the presence of population controls not ascertained for COVID-19 does not have a drastic impact in the association results.

The meta-analysis was performed using an inverse-variance weighting method in METAL[48]. Average allele frequency was calculated and variants with low imputation quality (Rsq<0.3) were filtered out, leaving 10,121,172 variants for meta-analysis.

Heterogeneity between studies was evaluated with the Cochran's-Q test. The inflation of results was assessed based on a genomic control (lambda).

Definition of the genetic risk loci and putative functional impact

Definition of lead variant and novel loci

To define the lead variants in the loci that were genome-wide significant, an LD-clumping was performed on the meta-analysis data using a threshold p-value<$5x10^{-8}$, clump distance=1500 kb, independence set at a threshold r^2=0.1 and used the SCOURGE cohort genotype data as LD reference panel. Independent loci were deemed as a novel finding if they met the following criteria: 1) p-value<$5x10^{-8}$ in the meta-analysis and p-value>$5x10^{-8}$ in the HGI B2 ALL meta-analysis or in the HGI B2 AMR and AFR and EUR analyses when considered by separate; 2) Cochran's Q-test for heterogeneity of effects is <$0.05/N_{loci}$, where N_{loci} is the number of independent variants with p<$5x10^{-8}$; and 3) the nearest gene has not been previously described in the latest HGIv7 update.

Annotation and initial mapping

Functional annotation was done with FUMA[49] for those variants with a p-value<$5x10^{-8}$ or in moderate-to-strong LD (r^2>0.6) with the lead variants, where the LD was calculated from the 1KGP AMR panel. Genetic risk loci were defined by collapsing LD-blocks within 250 kb. Then, genes, scaled CADD v1.4 scores, and RegulomeDB v1.1 scores were annotated for the resulting variants with ANNOVAR in FUMA[49]. Gene-based analysis was also performed using MAGMA[50] as implemented in FUMA, under the SNP-wide mean model using the 1KGP AMR reference panel. Significance was set at a threshold p<$2.66x10^{-6}$ (which assumes that variants can be mapped to a total of 18,817 genes).

FUMA allowed us to perform an initial gene mapping by two approaches: (1) positional mapping, which assigns variants to genes by physical distance using 10-kb windows; and (2) eQTL mapping based on GTEx v.8 data from whole blood, lungs, lymphocytes, and oesophagus mucosa tissues, establishing a False Discovery Rate (FDR) of 0.05 to declare significance for variant-gene pairs.

Subsequently, to assign the variants to the most likely gene driving the association, we refined the candidate genes by fine mapping the discovered regions and implementing functional mapping.

To conduct a Bayesian fine mapping, credible sets for the genetic loci considered novel findings were calculated on the results from each of the three meta-analyses to identify a subset of variants most likely containing the causal variant at 95% confidence level, assuming that there is a single causal variant and that it has been tested. We used *corrcoverage* (https://cran.rstudio.com/web/packages/corrcoverage/index.html) for R to calculate the posterior probabilities of the variant being causal for all variants with an r^2>0.1 with the leading SNP and within 1 Mb except for the novel variant in chromosome 19, for which we used a window of 0.5 Mb. Variants were added to the

credible set until the sum of the posterior probabilities was ≥0.95. VEP (https://www.ensembl.org/info/docs/tools/vep/index.html) and the V2G aggregate scoring from Open Targets Genetics (https://genetics.opentargets.org) were used to annotate the biological function of the variants contained in the fine-mapped credible sets

Colocalization analysis

We also conducted colocalization analyses to identify the putative causal genes that could act through the regulation of gene expression. FUMA's eQTL mapping enabled the identification of genes whose expression was associated with the variants in whole blood, lungs, lymphocytes, and oesophagus mucosa tissues. We combined this information with the VEP and V2G aggregate scoring to prioritize genes. For the fine-mapping regions, we included the variants within the calculated credible sets. In the cases where the fine mapping was unsuccessful, we considered variants within a 0.2 Mb window of the lead variant.

For each prioritized gene, we then run COLOC[51] to assess the evidence of colocalization between association signals and the eQTLs in each tissue, when at least one variant overlapped between them. COLOC estimates the posterior probability of two traits sharing the same causal variant in a locus. Prior probabilities of a variant being associated to COVID-19 phenotype (p1) and gene expression (p2) were set at $1x10^{-4}$, while pp2 was set at $1x10^{-6}$ as they are robust thresholds[52]. The posterior probability of colocalization (PP4) > 0.75 and a ratio PP4/PP3>3 were used as the criteria to support evidence of colocalization. Additionally, a threshold of PP4.SNP >0.5 was chosen for causal variant prioritization. In cases were colocalization of a single variant failed, we computed the 95% credible sets. The eQTL data was retrieved from GTEx v8 and only significant variant-gene pairs were considered in the analyses.

Colocalization in whole-blood was also performed using the recent published gene expression datasets derived from a cohort of African Americans, Puerto Ricans, and Mexican Americans (GALA II-SAGE)[53]. We used the results from the pooled cohort for the three discovered loci, and from the AFRHp5 (African genetic ancestry>50%) and IAMHp5 (Native American genetic ancestry>50%) cohorts for the risk loci in chromosomes 2 and 11. Results are shown in the Supplementary Table 10.

Sensitivity plots are shown in supplementary Figures 4 and 5.

Transcription-wide association studies

Transcriptome-wide association studies (TWAS) were conducted using the pretrained prediction models with MASHR-computed effect sizes on GTEx v8 datasets[54,55]. Results from the Latin-American meta-analysis were harmonized and integrated with the prediction models through S-PrediXcan[56] for lungs, whole blood, lymphocytes and oesophagus mucosa tissues. Statistical significance was set at p-value<0.05 divided by the number of genes that were tested for each tissue. Subsequently, we leveraged results for all 49 tissues and run a multi-tissue TWAS to improve power for association, as demonstrated recently[57]. TWAS was also conducted with the MASHR models for whole-blood in the pooled admixed AMR from the GALA and SAGE studies[53].

Cross-population meta-analyses

We conducted two additional meta-analyses to investigate the ability of combining populations to replicate our discovered risk loci. This methodology enabled the comparison of effects and the significance of associations in the novel risk loci between the results from analyses that included or excluded other population groups.

The first meta-analysis comprised the five populations analysed within HGI (B2-ALL). Additionally, to evaluate the three GIA components within the SCOURGE Latin-

American cohort[58], we conducted a meta-analysis of the admixed AMR, EUR, and AFR cohorts (B2). All summary statistics were retrieved from the HGI repository. We applied the same meta-analysis methodology and filters as in the admixed AMR meta-analysis. Novel variants from these meta-analyses were fine-mapped and colocalized with gene expression.

Cross-population Polygenic Risk Score

A polygenic risk score (PGS) for critical COVID-19 was derived combining the variants associated with hospitalization or disease severity that have been discovered to date. We curated a list of lead variants that were: 1) associated to either severe disease or hospitalization in the latest HGIv7 release[1] (using the hospitalization weights); or 2) associated to severe disease in the latest GenOMICC meta-analysis[2] that were not reported in the latest HGI release. A total of 49 markers were used in the PGS model (see supplementary Table 13) since two variants were absent from our study.

Scores were calculated and normalized for the SCOURGE Latin-American cohort with PLINK 1.9. This cross-ancestry PGS was used as a predictor for hospitalization (COVID-19 positive that were hospitalized *vs.* COVID-19 positive that did not necessitate hospital admission) by fitting a logistic regression model. Prediction accuracy for the PGS was assessed by performing 500 bootstrap resamples of the increase in the pseudo-R-squared. We also divided the sample in deciles and percentiles to assess risk stratification. The models were fit for the dependent variable adjusting for sex, age, the first 10 PCs, and the sampling region (in the Admixed AMR cohort) with and without the PGS, and the partial pseudo-R2 was computed and averaged among the resamples.

A clinical severity scale was used in a multinomial regression model to further evaluate the power of this cross-ancestry PGS for risk stratification. This severity strata were defined as follows: 0) asymptomatic; 1) mild, that is, with symptoms, but without pulmonary infiltrates or need of oxygen therapy; 2) moderate, that is, with pulmonary infiltrates affecting <50% of the lungs or need of supplemental oxygen therapy; 3) severe disease, that is with hospital admission and PaO_2<65 mmHg or SaO_2<90%, PaO_2/FiO_2<300, SaO_2/FiO_2<440, dyspnea, respiratory frequency≥22 bpm, and infiltrates affecting >50% of the lungs; and 4) critical disease, that is with an admission to the ICU or need of mechanical ventilation (invasive or non-invasive). We also included the novel risk variants as predictors alongside the PRS to determine if they provided increased prediction ability.

Data availability

Summary statistics from the SCOURGE Latin-American GWAS will be available at https://github.com/CIBERER/Scourge-COVID19.

Funding

Instituto de Salud Carlos III (COV20_00622 to A.C., COV20/00792 to M.B., COV20_00181 to C.A., COV20_1144 to M.A.J.S. and A.F.R., PI20/00876 to C.F.); European Union (ERDF) 'A way of making Europe'. Fundación Amancio Ortega, Banco de Santander (to A.C.), Estrella de Levante S.A. and Colabora Mujer Association (to E.G.-N.) and Obra Social La Caixa (to R.B.); Agencia Estatal de Investigación (RTC-2017-6471-1 to C.F.), Cabildo Insular de Tenerife (CGIEU0000219140 'Apuestas científicas del ITER para colaborar en la lucha contra la COVID-19' to C.F.)

and Fundación Canaria Instituto de Investigación Sanitaria de Canarias (PIFIISC20/57 to C.F.).

SD-DA was supported by a Xunta de Galicia predoctoral fellowship.

Author contributions

Study design: RC, AC, CF. Data collection: SCOURGE cohort group. Data analysis: SD-DA, RC, ADL, CF, JML-S. Interpretation: SD-DA, RC, ADL. Drafting of the manuscript: SD-DA, RC, ADL, CF, AR-M, AC. Critical revision of the manuscript: SD-DA, RC, ADL, AC, CF, JAR, AR-M, PL. Approval of the final version of the publication: all co-authors.

Acknowledgements

The contribution of the Centro National de Genotipado (CEGEN), and Centro de Supercomputación de Galicia (CESGA) for funding this project by providing supercomputing infrastructures, is also acknowledged. Authors are also particularly grateful for the supply of material and the collaboration of patients, health professionals from participating centers and biobanks. Namely Biobanc-Mur, and biobancs of the Complexo Hospitalario Universitario de A Coruña, Complexo Hospitalario Universitario de Santiago, Hospital Clínico San Carlos, Hospital La Fe, Hospital Universitario Puerta de Hierro Majadahonda—Instituto de Investigación Sanitaria Puerta de Hierro—Segovia de Arana, Hospital Ramón y Cajal, IDIBGI, IdISBa, IIS Biocruces Bizkaia, IIS Galicia Sur. Also biobanks of the Sistema de Salud de Aragón, Sistema Sanitario Público de Andalucía, and Banco Nacional de ADN.

References

628 1. Initiative, T. C.-19 H. G. & Ganna, A. A second update on mapping the human genetic
629 architecture of COVID-19. 2022.12.24.22283874 Preprint at
630 https://doi.org/10.1101/2022.12.24.22283874 (2023).

631 2. GWAS and meta-analysis identifies 49 genetic variants underlying critical COVID-19 |
632 Nature. https://www.nature.com/articles/s41586-023-06034-3.

633 3. Niemi, M. E. K. *et al.* Mapping the human genetic architecture of COVID-19. *Nature*
634 **600**, 472–477 (2021).

635 4. Popejoy, A. B. & Fullerton, S. M. Genomics is failing on diversity. *Nature* **538**, 161–164
636 (2016).

637 5. Sirugo, G., Williams, S. M. & Tishkoff, S. A. The Missing Diversity in Human Genetic
638 Studies. *Cell* **177**, 26–31 (2019).

639 6. Li, Y. R. & Keating, B. J. Trans-ethnic genome-wide association studies: advantages and
640 challenges of mapping in diverse populations. *Genome Med.* **6**, 91 (2014).

641 7. Rosenberg, N. A. *et al.* Genome-wide association studies in diverse populations. *Nat.*
642 *Rev. Genet.* **11**, 356–366 (2010).

643 8. Kwok, A. J., Mentzer, A. & Knight, J. C. Host genetics and infectious disease: new tools,
644 insights and translational opportunities. *Nat. Rev. Genet.* **22**, 137–153 (2021).

645 9. Karlsson, E. K., Kwiatkowski, D. P. & Sabeti, P. C. Natural selection and infectious
646 disease in human populations. *Nat. Rev. Genet.* **15**, 379–393 (2014).

647 10. Namkoong, H. *et al.* DOCK2 is involved in the host genetics and biology of severe
648 COVID-19. *Nature* **609**, 754–760 (2022).

649 11. Bastard, P. *et al.* A loss-of-function IFNAR1 allele in Polynesia underlies severe viral
650 diseases in homozygotes. *J. Exp. Med.* **219**, e20220028 (2022).

651 12. Duncan, C. J. A. *et al.* Life-threatening viral disease in a novel form of autosomal
652 recessive IFNAR2 deficiency in the Arctic. *J. Exp. Med.* **219**, e20212427 (2022).

653 13. Peterson, R. E. *et al.* Genome-wide Association Studies in Ancestrally Diverse
654 Populations: Opportunities, Methods, Pitfalls, and Recommendations. *Cell* **179**, 589–603
655 (2019).

656 14. Mester, R. *et al.* Impact of cross-ancestry genetic architecture on GWAS in admixed
657 populations. 2023.01.20.524946 Preprint at https://doi.org/10.1101/2023.01.20.524946
658 (2023).

659 15. Tractor uses local ancestry to enable the inclusion of admixed individuals in GWAS and
660 to boost power | Nature Genetics. https://www.nature.com/articles/s41588-020-00766-y.

661 16. Cruz, R. *et al.* Novel genes and sex differences in COVID-19 severity. *Hum. Mol. Genet.*
662 **31**, 3789–3806 (2022).

663 17. Degenhardt, F. *et al.* Detailed stratified GWAS analysis for severe COVID-19 in four
664 European populations. *Hum. Mol. Genet.* **31**, 3945–3966 (2022).

665 18. Whole-genome sequencing reveals host factors underlying critical COVID-19 | Nature.
666 https://www.nature.com/articles/s41586-022-04576-6.

19. Evolution-based screening enables genome-wide prioritization and discovery of DNA repair genes | PNAS. https://www.pnas.org/doi/full/10.1073/pnas.1906559116.

20. Human Noxin is an anti-apoptotic protein in response to DNA damage of A549 non-small cell lung carcinoma - Won - 2014 - International Journal of Cancer - Wiley Online Library. https://onlinelibrary.wiley.com/doi/10.1002/ijc.28600.

21. Gioia, U. *et al.* SARS-CoV-2 infection induces DNA damage, through CHK1 degradation and impaired 53BP1 recruitment, and cellular senescence. *Nat. Cell Biol.* **25**, 550–564 (2023).

22. Im, J.-Y. *et al.* DDIAS promotes STAT3 activation by preventing STAT3 recruitment to PTPRM in lung cancer cells. *Oncogenesis* **9**, 1–11 (2020).

23. Im, J.-Y., Kang, M.-J., Kim, B.-K. & Won, M. DDIAS, DNA damage-induced apoptosis suppressor, is a potential therapeutic target in cancer. *Exp. Mol. Med.* 1–7 (2023) doi:10.1038/s12276-023-00974-6.

24. Angeli, F. *et al.* The spike effect of acute respiratory syndrome coronavirus 2 and coronavirus disease 2019 vaccines on blood pressure. *Eur. J. Intern. Med.* **109**, 12–21 (2023).

25. Silva-Aguiar, R. P. *et al.* Role of the renin-angiotensin system in the development of severe COVID-19 in hypertensive patients. *Am. J. Physiol.-Lung Cell. Mol. Physiol.* **319**, L596–L602 (2020).

26. Li, Y. *et al.* The emerging role of ISWI chromatin remodeling complexes in cancer. *J. Exp. Clin. Cancer Res.* **40**, 346 (2021).

27. The Dendritic Cell Receptor for Endocytosis, Dec-205, Can Recycle and Enhance Antigen Presentation via Major Histocompatibility Complex Class II–Positive Lysosomal Compartments | Journal of Cell Biology | Rockefeller University Press. https://rupress.org/jcb/article/151/3/673/21295/The-Dendritic-Cell-Receptor-for-Endocytosis-Dec.

28. Sims, A. C. *et al.* Release of Severe Acute Respiratory Syndrome Coronavirus Nuclear Import Block Enhances Host Transcription in Human Lung Cells. *J. Virol.* **87**, 3885–3902 (2013).

29. A Network Integration Approach to Predict Conserved Regulators Related to Pathogenicity of Influenza and SARS-CoV Respiratory Viruses | PLOS ONE. https://journals.plos.org/plosone/article?id=10.1371/journal.pone.0069374.

30. Gómez-Carballa, A. *et al.* A multi-tissue study of immune gene expression profiling highlights the key role of the nasal epithelium in COVID-19 severity. *Environ. Res.* **210**, 112890 (2022).

31. Policard, M., Jain, S., Rego, S. & Dakshanamurthy, S. Immune characterization and profiles of SARS-CoV-2 infected patients reveals potential host therapeutic targets and SARS-CoV-2 oncogenesis mechanism. *Virus Res.* **301**, 198464 (2021).

32. Wei, J. *et al.* Genome-wide CRISPR Screens Reveal Host Factors Critical for SARS-CoV-2 Infection. *Cell* **184**, 76-91.e13 (2021).

33. Wei, J. *et al.* Pharmacological disruption of mSWI/SNF complex activity restricts SARS-CoV-2 infection. *Nat. Genet.* **55**, 471–483 (2023).

706 34. Pereira, A. C. *et al.* Genetic risk factors and COVID-19 severity in Brazil: results from
707 BRACOVID study. *Hum. Mol. Genet.* **31**, 3021–3031 (2022).

708 35. Zhu, X. *et al.* ZBTB7A promotes virus-host homeostasis during human coronavirus 229E
709 infection. *Cell Rep.* **41**, 111540 (2022).

710 36. Gupta, S. *et al.* Emerging role of ZBTB7A as an oncogenic driver and transcriptional
711 repressor. *Cancer Lett.* **483**, 22–34 (2020).

712 37. Yoneyama, M. *et al.* Direct triggering of the type I interferon system by virus infection:
713 activation of a transcription factor complex containing IRF-3 and CBP/p300. *EMBO J.* **17**, 1087–
714 1095 (1998).

715 38. Yang, Q. *et al.* SARS-CoV-2 infection activates CREB/CBP in cellular cyclic AMP-
716 dependent pathways. *J. Med. Virol.* **95**, e28383 (2023).

717 39. Harris, P. A. *et al.* Research electronic data capture (REDCap)—A metadata-driven
718 methodology and workflow process for providing translational research informatics support. *J.*
719 *Biomed. Inform.* **42**, 377–381 (2009).

720 40. Harris, P. A. *et al.* The REDCap consortium: Building an international community of
721 software platform partners. *J. Biomed. Inform.* **95**, 103208 (2019).

722 41. Purcell, S. *et al.* PLINK: A Tool Set for Whole-Genome Association and Population-
723 Based Linkage Analyses. *Am. J. Hum. Genet.* **81**, 559–575 (2007).

724 42. Alexander, D. H., Novembre, J. & Lange, K. Fast model-based estimation of ancestry in
725 unrelated individuals. *Genome Res.* **19**, 1655–1664 (2009).

726 43. Auton, A. *et al.* A global reference for human genetic variation. *Nature* **526**, 68–74
727 (2015).

728 44. Mao, X. *et al.* A Genomewide Admixture Mapping Panel for Hispanic/Latino
729 Populations. *Am. J. Hum. Genet.* **80**, 1171–1178 (2007).

730 45. Wojcik, G. L. *et al.* Genetic analyses of diverse populations improves discovery for
731 complex traits. *Nature* **570**, 514–518 (2019).

732 46. Zheng, X. & Davis, J. W. SAIGEgds—an efficient statistical tool for large-scale PheWAS
733 with mixed models. *Bioinformatics* **37**, 728–730 (2021).

734 47. Zhou, W. *et al.* Efficiently controlling for case-control imbalance and sample
735 relatedness in large-scale genetic association studies. *Nat. Genet.* **50**, 1335–1341 (2018).

736 48. METAL: fast and efficient meta-analysis of genomewide association scans |
737 Bioinformatics | Oxford Academic.
738 https://academic.oup.com/bioinformatics/article/26/17/2190/198154.

739 49. Watanabe, K., Taskesen, E., van Bochoven, A. & Posthuma, D. Functional mapping and
740 annotation of genetic associations with FUMA. *Nat. Commun.* **8**, 1826 (2017).

741 50. MAGMA: Generalized Gene-Set Analysis of GWAS Data | PLOS Computational Biology.
742 https://journals.plos.org/ploscompbiol/article?id=10.1371/journal.pcbi.1004219.

743 51. Giambartolomei, C. *et al.* Bayesian Test for Colocalisation between Pairs of Genetic
744 Association Studies Using Summary Statistics. *PLOS Genet.* **10**, e1004383 (2014).

745 52. Wallace, C. Eliciting priors and relaxing the single causal variant assumption in
746 colocalisation analyses. *PLOS Genet.* **16**, e1008720 (2020).

747 53. Kachuri, L. *et al.* Gene expression in African Americans, Puerto Ricans and Mexican
748 Americans reveals ancestry-specific patterns of genetic architecture. *Nat. Genet.* **55**, 952–963
749 (2023).

750 54. Barbeira, A. N. *et al.* Exploiting the GTEx resources to decipher the mechanisms at
751 GWAS loci. *Genome Biol.* **22**, 49 (2021).

752 55. Barbeira, A. N. *et al.* GWAS and GTEx QTL integration. (2019)
753 doi:10.5281/zenodo.3518299.

754 56. Barbeira, A. N. *et al.* Exploring the phenotypic consequences of tissue specific gene
755 expression variation inferred from GWAS summary statistics. *Nat. Commun.* **9**, 1825 (2018).

756 57. Barbeira, A. N. *et al.* Integrating predicted transcriptome from multiple tissues
757 improves association detection. *PLOS Genet.* **15**, e1007889 (2019).

758 58. Genome-wide patterns of population structure and admixture among Hispanic/Latino
759 populations | PNAS. https://www.pnas.org/doi/10.1073/pnas.0914618107?url_ver=Z39.88-
760 2003&rfr_id=ori:rid:crossref.org&rfr_dat=cr_pub%20%200pubmed.

761

762

763 Table 1. Demographic characteristics of the SCOURGE Latin-American cohort.

Variable	Non Hospitalized N = 1,887	Hospitalized N = 1,608
Age – mean years ± SD	39.1 ± 11.9	54.1 ±14.5
Sex - N (%)		
Female (%)	1253 (66.4)	668 (41.5)
GIA* – % mean ±SD		
European	54.4 ±16.2	39.4 ± 20.7
African	15.3 ± 12.7	9.1 ± 11.6
Native American	30.3 ± 19.8	51.46 ± 26.5
Comorbidities - N (%)		
Vascular/endocrinological	488 (25.9)	873 (54.3)
Cardiac	60 (3.2)	150 (9.3)
Nervous	15 (0.8)	61 (3.8)
Digestive	14 (0.7)	33 (2.0)
Onco-hematological	21 (1.1)	48 (3.00)

Respiratory	76 (4.0)	118 (7.3)

*Global genetic inferred ancestry.

Table 2. Lead independent variants in the admixed AMR GWAS meta-analysis.

SNP rsID	*chr:pos*	*EA*	*NEA*	*OR (95% CI)*	*P-value*	*EAF cases*	*EAF controls*	*Nearest gene*
rs13003835	2:159407982	T	C	1.20 (1.12-1.27)	3.66E-08	0.563	0.429	*BAZ2B*
rs35731912	3:45848457	T	C	1.65 (1.47-1.85)	6.30E-17	0.087	0.056	*LZTFL1*
rs2477820	6:41535254	A	T	0.84 (0.79-0.89)	1.89E-08	0.453	0.517	*FOXP4-AS1*
rs77599934	11:82906875	G	A	2.27 (1.7-3.04)	2.26E-08	0.016	0.011	*DDIAS*

EA: effect allele; NEA: non-effect allele; EAF: effect allele frequency in the SCOURGE study.

Table 3. Novel variants in the SC-HGI$_{ALL}$ and SC-HGI$_{3POP}$ meta-analyses (with respect to HGIv7). Independent signals after LD clumping.

SNP rsID	*chr:pos*	*EA*	*NEA*	*OR (95% CI)*	*P-value*	*Nearest gene*	*Analysis*
rs76564172	16:3892266	T	G	1.31 (1.19-1.44)	9.64E-09	*CREBBP*	SC-HGI$_{3POP}$
rs66833742	19:4063488	T	C	0.94 (0.92-0.96)	1.89E-08	*ZBTB7A*	SC-HGI$_{3POP}$
rs66833742	19:4063488	T	C	0.94 (0.92-0.96)	2.50E-08	*ZBTB7A*	SC-HGI$_{ALL}$
rs2876034	20:6492834	A	T	0.95 (0.93-0.97)	2.83E-08	*CASC20*	SC-HGI$_{ALL}$

EA: effect allele; NEA: non-effect allele.

Figure 1. Flow chart of this study.

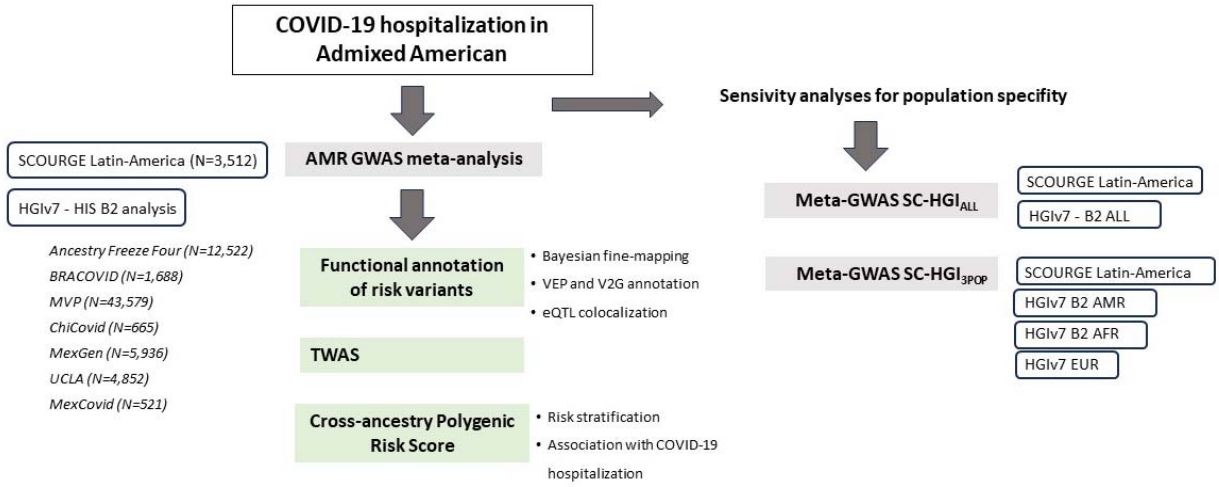

774

775

776

777

778 Figure 2. A) Manhattan plot for the admixed AMR GWAS meta-analysis. Probability
779 thresholds at $p=5x10^{-8}$ and $p=5x10^{-5}$ are indicated by the horizontal lines. Genome-wide
780 significant associations with COVID-19 hospitalizations were found in chromosome 2
781 (within *BAZ2B*), chromosome 3 (within *LZTFL1*), chromosome 6 (within *FOXP4*), and
782 chromosome 11 (within *DDIAS*). A Quantile-Quantile plot is shown in supplementary
783 Figure 2. B) Regional association plots for rs1003835 at chromosome 2 and rs77599934
784 at chromosome 11; C) Allele frequency distribution across The 1000 Genomes Project
785 populations for the lead variants rs1003835 and rs77599934.

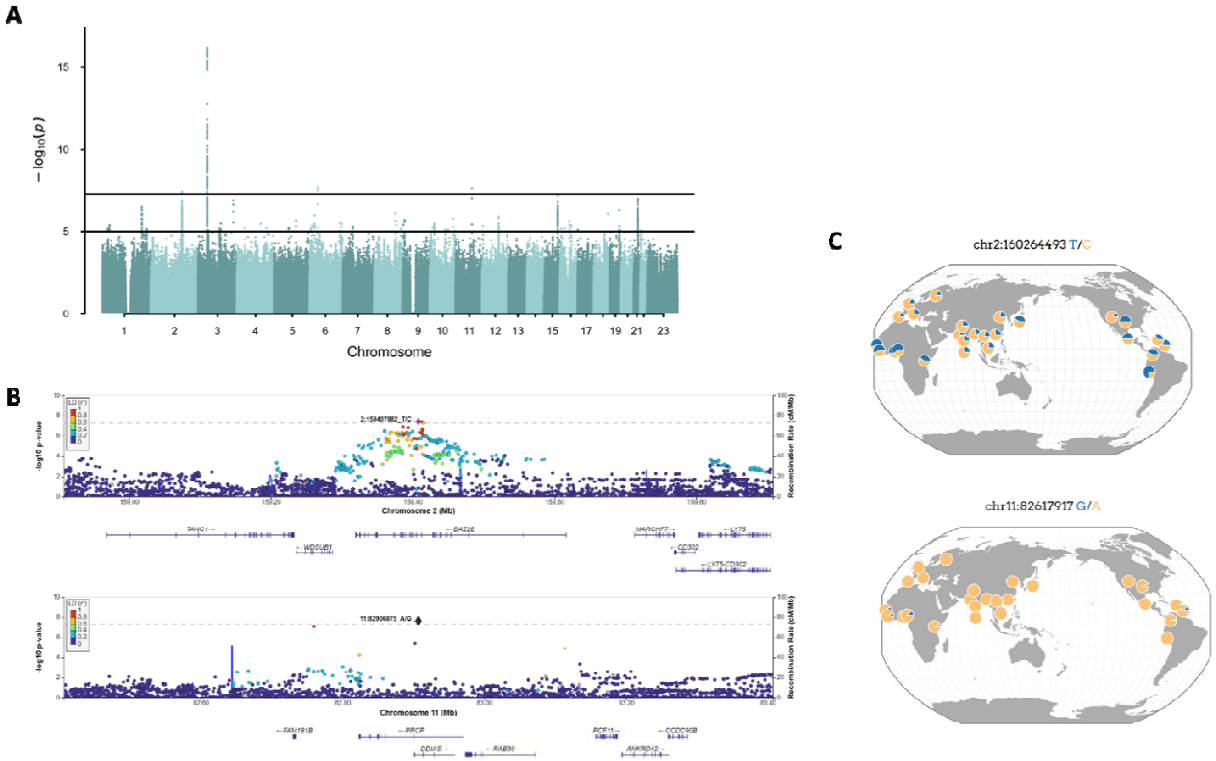

Figure 3. Forest plot showing effect sizes and the corresponding confidence intervals for the sentinel variants identified in the AMR meta-analysis across populations. All beta values with their corresponding CIs were retrieved from the B2 population-specific meta-analysis from the HGI v7 release, except for AMR, for which the beta value and IC from the HGI_{AMR}-SCOURGE meta-analysis is represented.

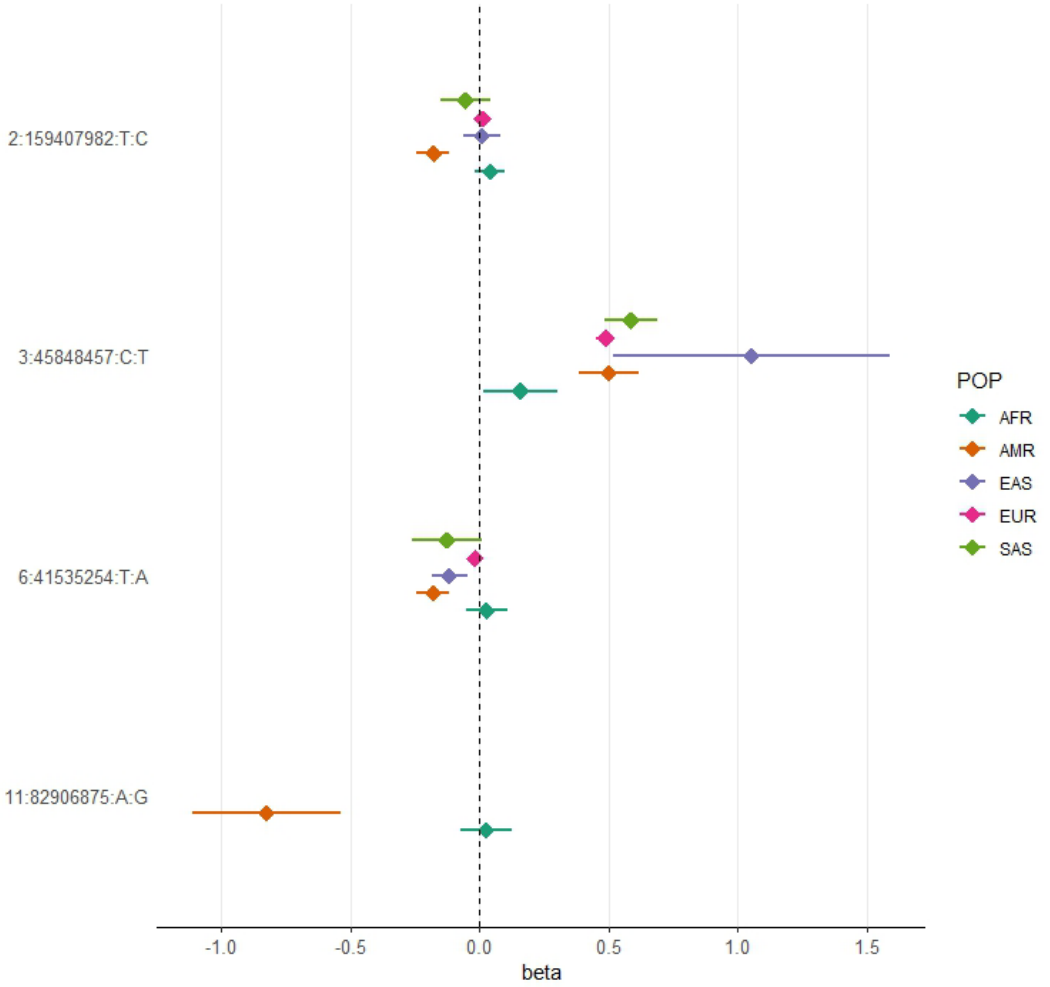

794

795

796 Figure 4. (A) Polygenic risk stratified by PGS deciles comparing each risk group
797 against the lowest risk group (OR-95%CI); (B) Distribution of the PGS scores in each
798 of the severity scale classes (0-Asymptomatic, 1-Mild disease, 2-Moderate disease, 3-
799 Severe disease, 4-Critical disease).

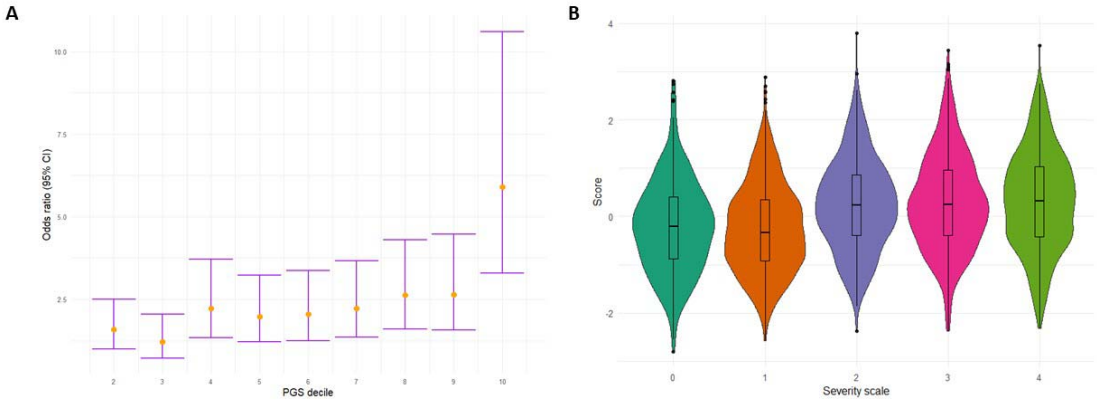

Supplementary Material for: Novel risk loci for COVID-19 hospitalization among admixed American populations

Supplementary Tables are provided in a separate excel file

Supplementary figures

Supplementary Figure 1. Global Genetic Inferred Ancestry (GIA) composition in the SCOURGE Latin-American cohort. European (EUR), African (AFR) and Native American (AMR) GIA was derived with ADMIXTURE from a reference panel composed of Aymaran, Mayan, Nahuan, and Quechuan individuals of Native-American genetic ancestry and randomly selected samples from the EUR and AFR 1KGP populations. The colours represent the different geographical sampling regions from which the admixed American individuals from SCOURGE were recruited.

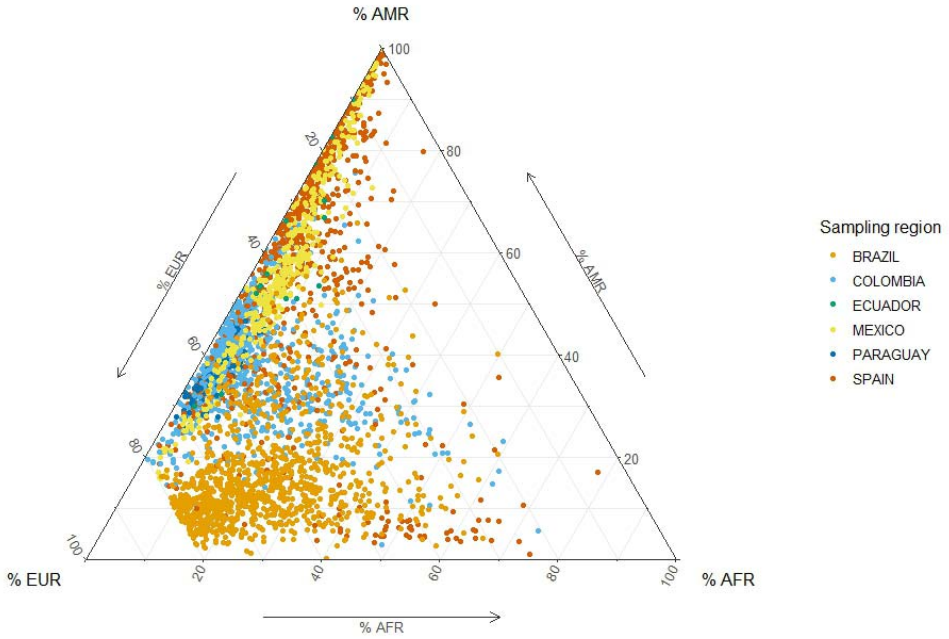

814

815

816 **Supplementary Figure 2. Quantile-Quantile plot for the AMR GWAS meta-**
817 **analysis.** A lambda inflation factor of 1.015 was obtained.

818

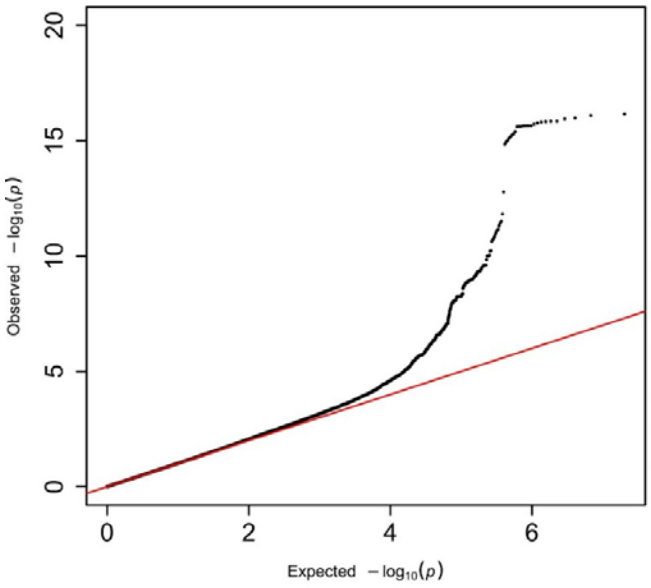

819

820

Supplementary Figure 3. Regional association plots for the fine mapped loci in chromosomes 2 (upper panel) and 16 (lower panel). Coloured in red, the variants allocated to the credible set at the 95% confidence according to the Bayesian fine mapping. In blue, the sentinel variant.

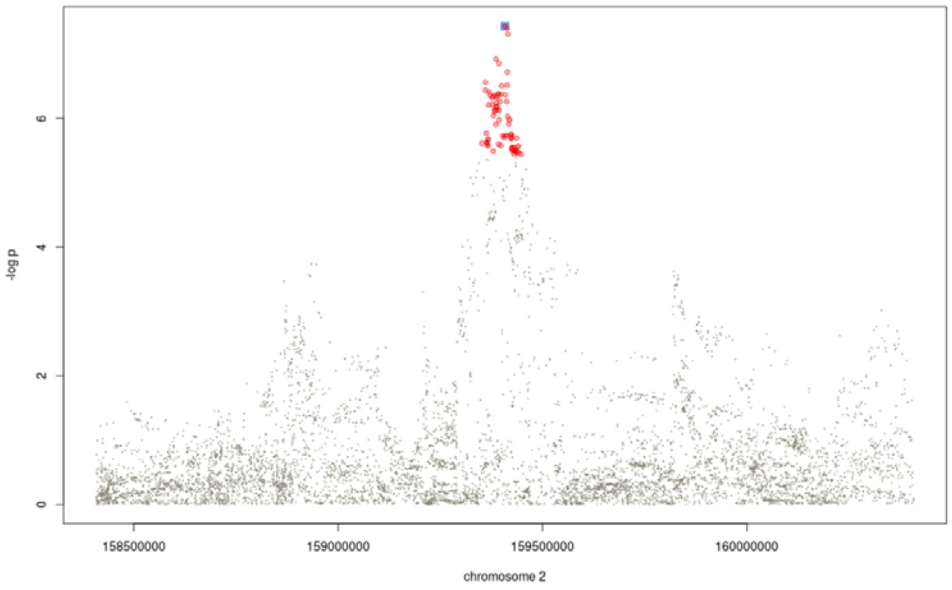

834

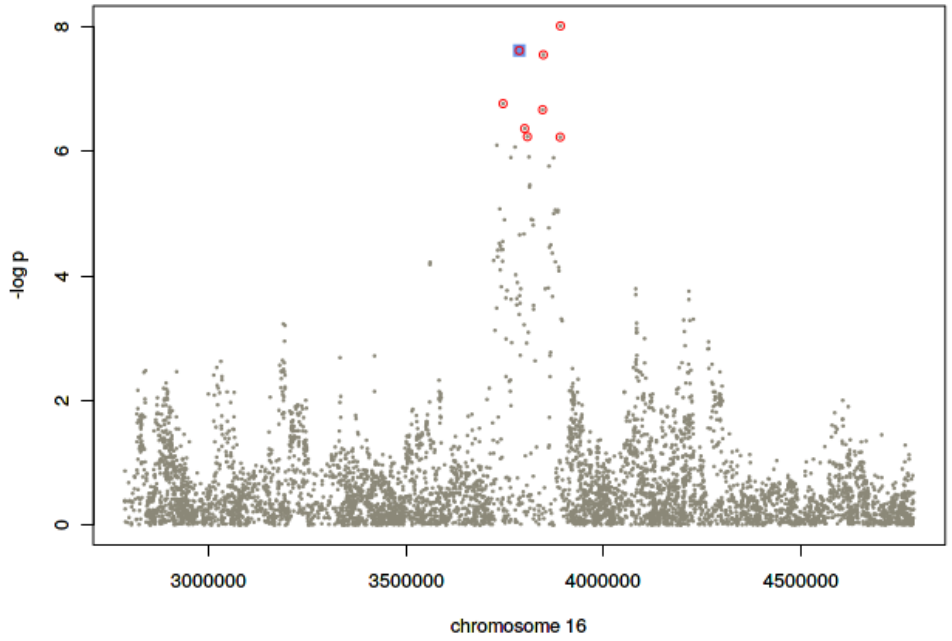

835

836

837 **Supplementary Figure 4. Sensitivity plots from COLOC with expression data from**
838 **GTEx v8.** The range of p12 values (probability that a SNP is associated with both
839 traits) for which the rule H_4>0.7 is supported is shown in green in the right plots for
840 each analysis. Plots in the left represent the variants included in the risk region common
841 to both traits along their individual association -log10(p-values) for each trait, whereas
842 the shading shows the posterior probability that the SNP is causal given H_4 is true. Trait
843 1 corresponds to COVID-19 hospitalization, while trait 2 corresponds to gene
844 expression in each analysis.

845

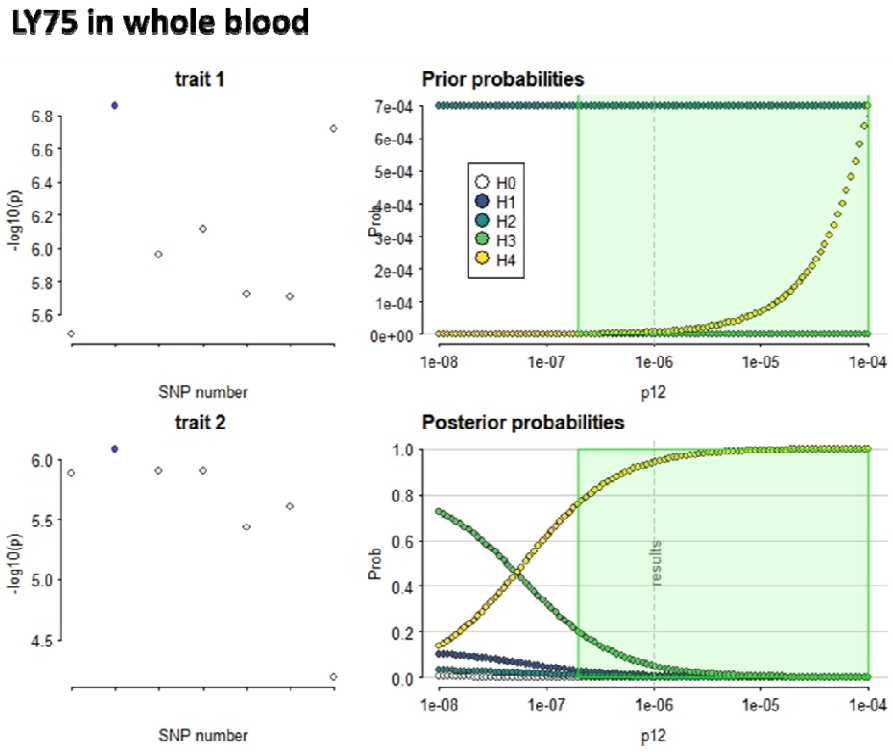

846

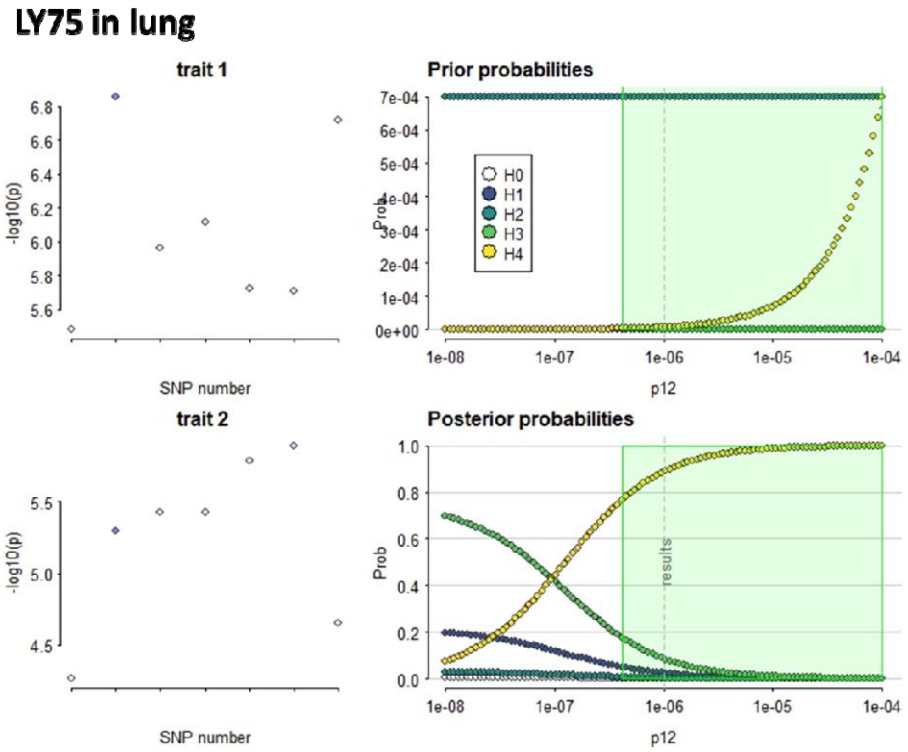

847

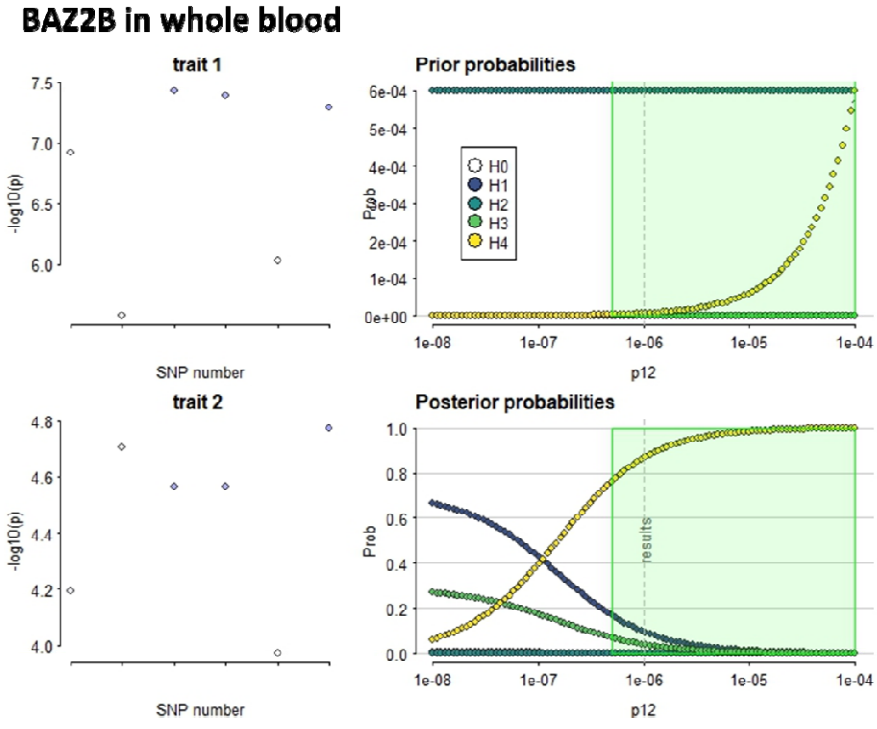

848

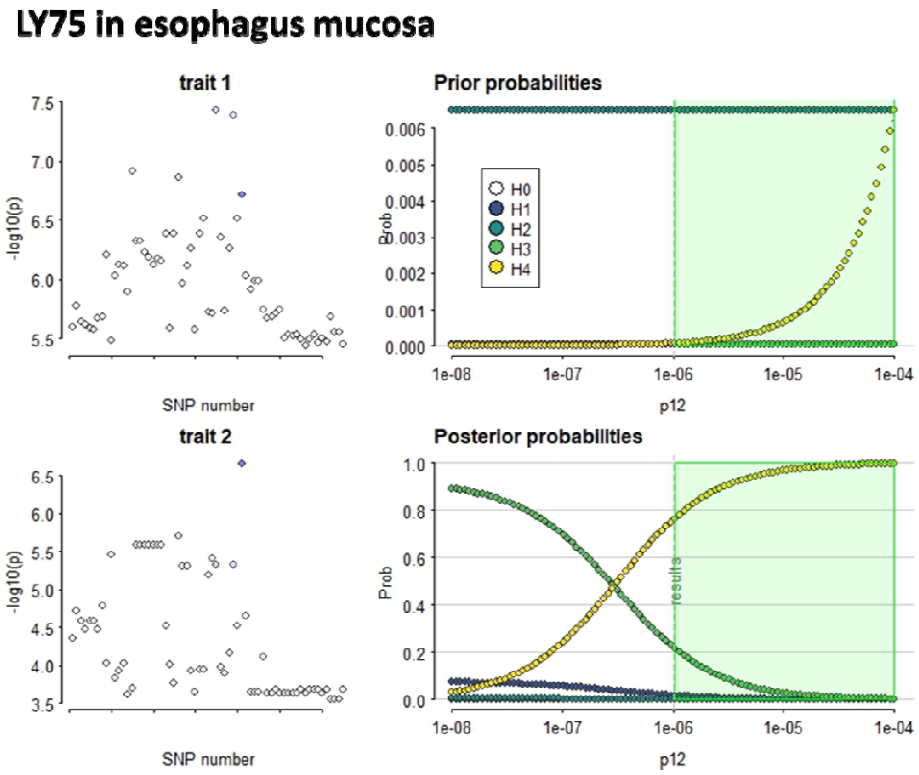

Supplementary Figure 5. Sensitivity plots from COLOC with whole blood expression data from the GALA and SAGE II studies in AMR individuals. *AFRhp5* corresponds to the expression dataset computed in individuals with high African ancestries; *AMRhp5* corresponds to the expression dataset computed individuals with high AMR ancestries; *pooled* corresponds to the dataset computed with the total of individuals from the study. In the right, the plots show in green the range of p12 values (probability that a SNP is associated with both traits) for which the rule H_4>0.7 is supported. Plots in the left represent the variants included in the risk region common to both traits along their individual association -log10(p-values) for each trait, whereas the shading shows the posterior probability that the SNP is causal given H_4 is true. Trait 1 corresponds to COVID-19 hospitalization, while trait 2 corresponds to gene expression.

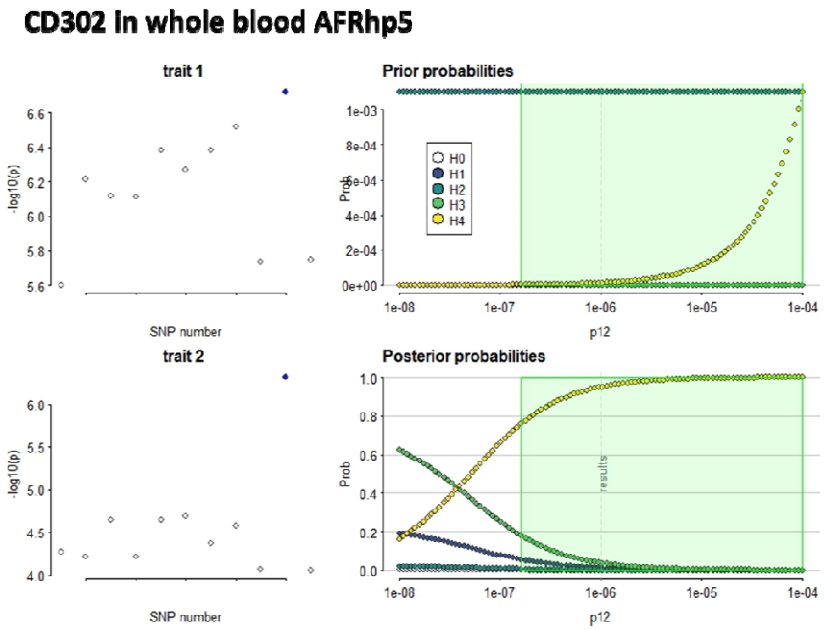

862

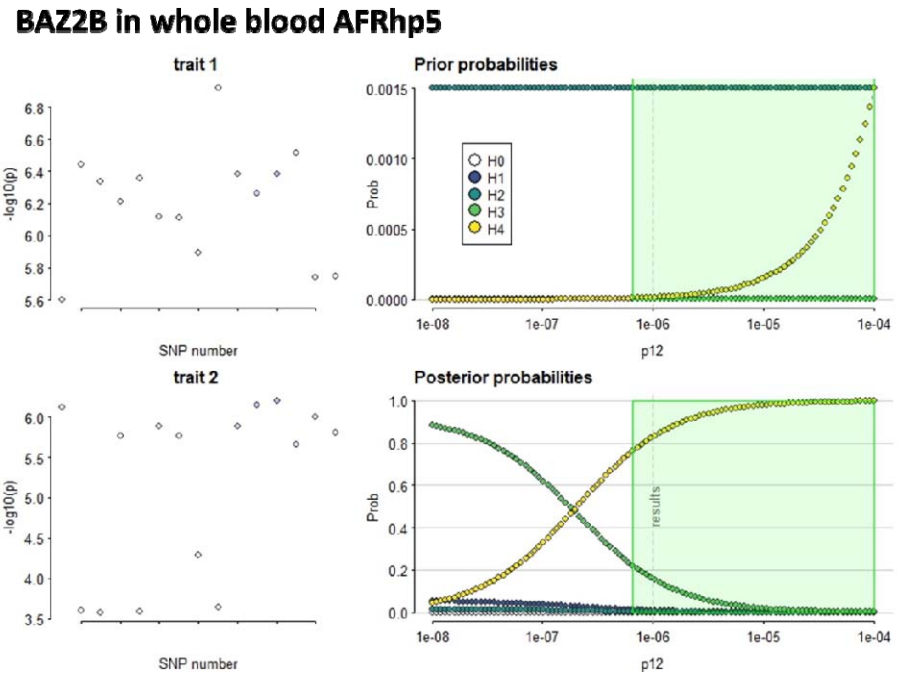

863

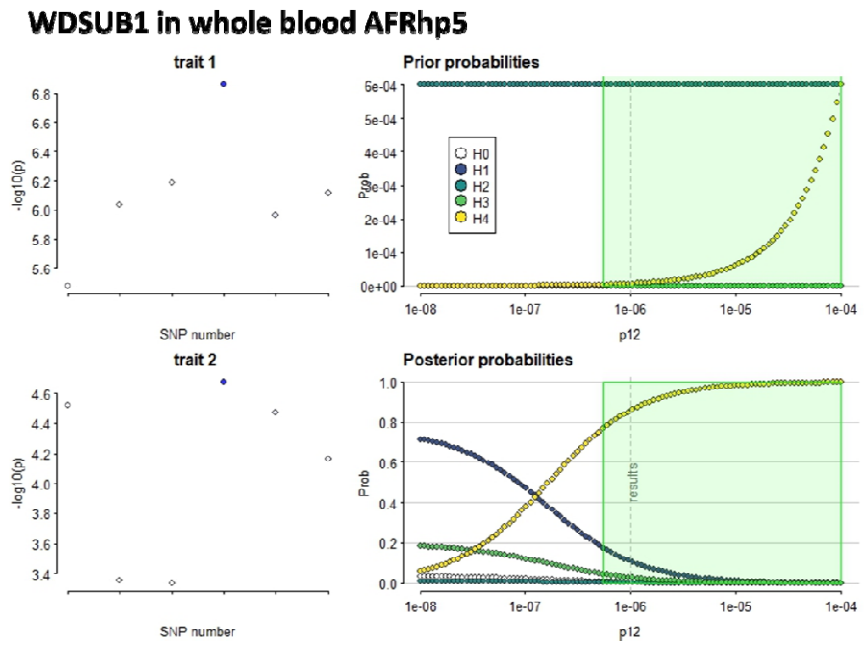

864

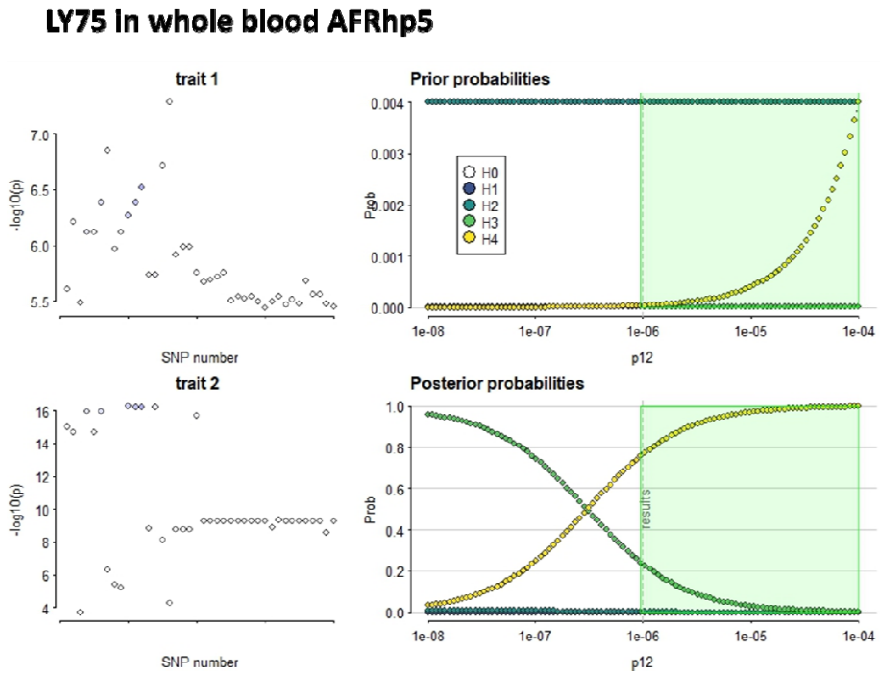

865

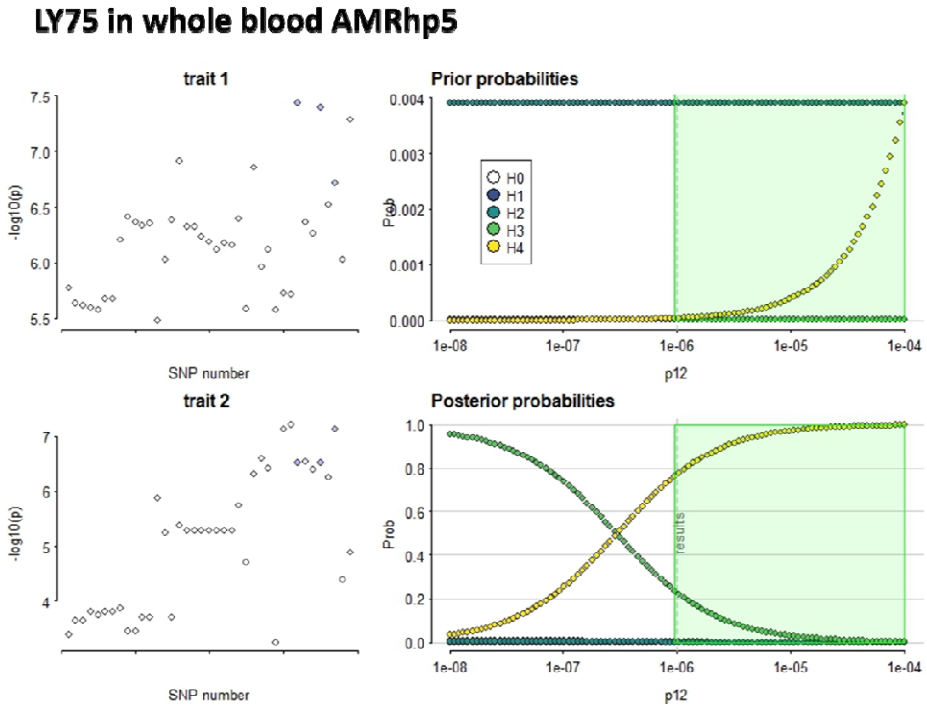

866

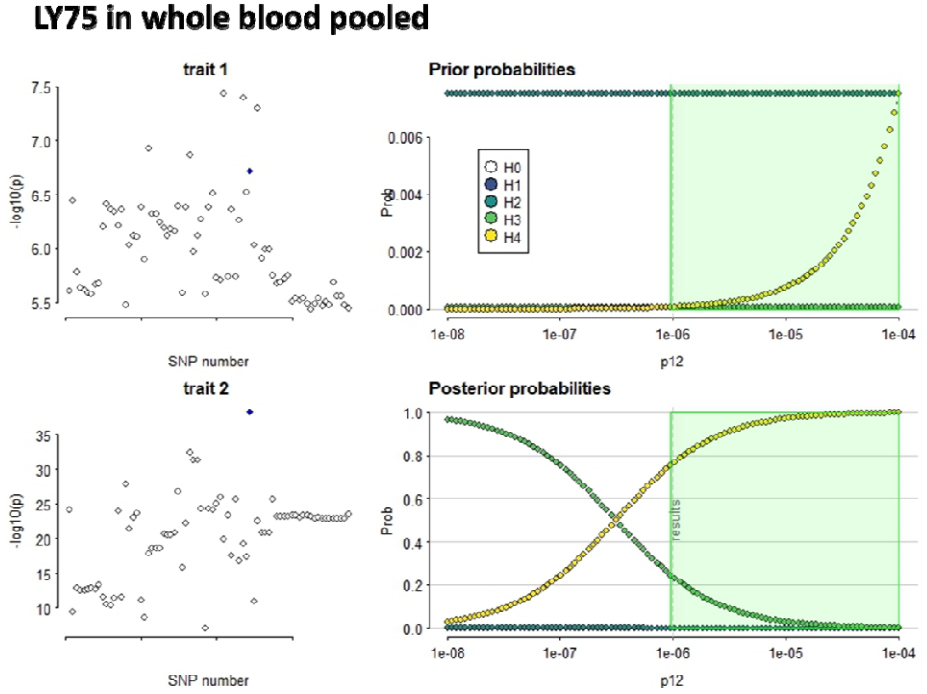

867

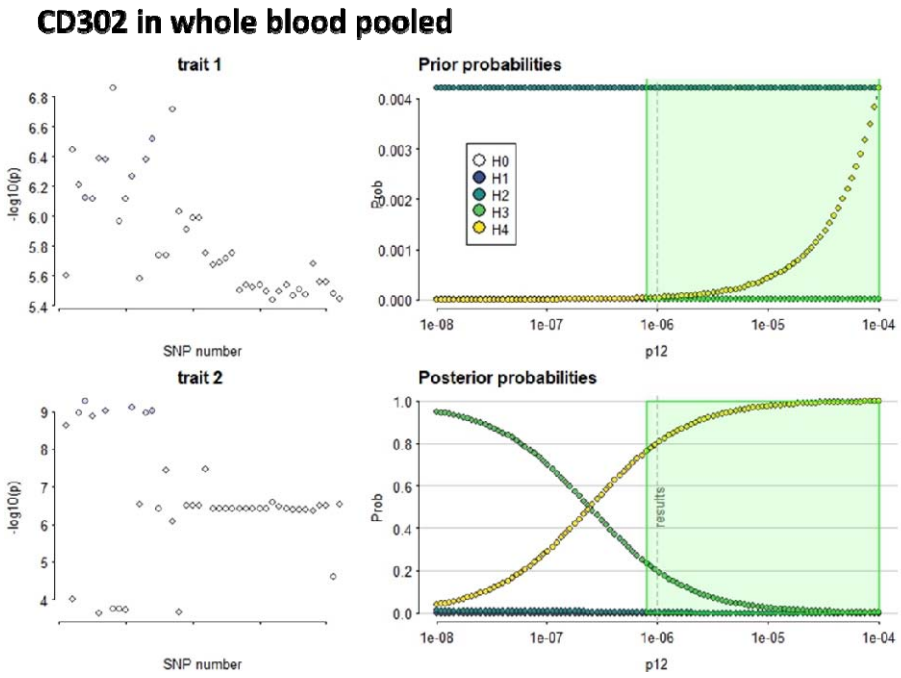

868

869

870

871 **Supplementary Figure 6. Gene-tissue pairs for which either rs1003835 or**
872 **rs60606421 are significant eQTLs at FDR<0.05 (data retrieved from**
873 **https://gtexportal.org/home/snp/).** rs1003835 (chromosome 2) maps to *BAZ2B*, *LY75*,
874 and *PLA2R* genes. As for the lead variant of chromosome 11, rs77599934, since it was
875 not an eQTL, we used an LD proxy variant (rs60606421). *DDIAS* and *PRCP* genes map
876 closely to this variant. NES and p-values correspond to the normalized effect size (and
877 direction) of eQTL-gene associations and the p-value for the tissue, respectively.

878

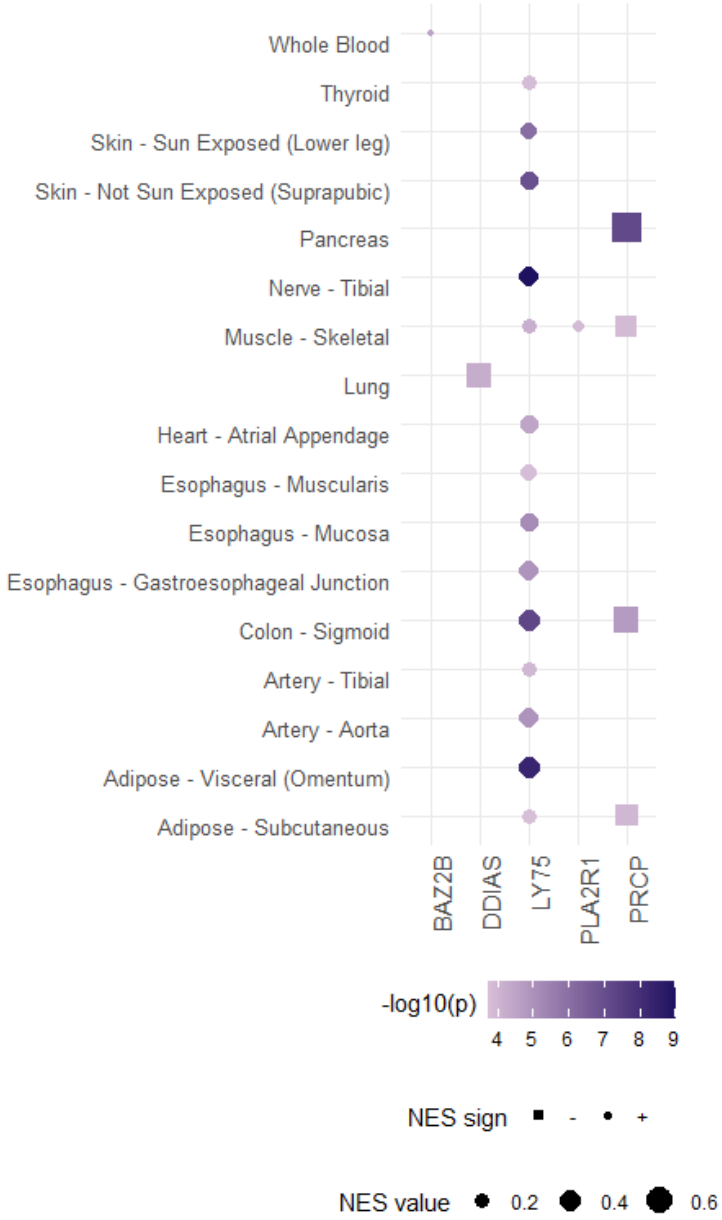

879

880

881

882